


## Thermodynamics and the pairon model for cuprates

Jeffery L. Tallon<sup>✉\*</sup> and James G. Storey<sup>✉</sup>

Robinson Research Institute, and MacDiarmid Institute for Advanced Materials and Nanotechnology,  
Victoria University of Wellington, P.O. Box 33436, Lower Hutt 5046, New Zealand

 (Received 27 November 2022; revised 18 January 2023; accepted 19 January 2023; published 22 February 2023)

Two recent papers explore the idea of “pairons” (incoherent bound pairs above  $T_c$ ) as a model for the pseudogap in cuprate high- $T_c$  superconductors. From this model the authors calculate the resultant electronic specific heat and static magnetic susceptibility. At elevated temperature the pairons thermally unbind causing a broad peak in the specific heat, additional to the second-order peak at  $T_c$  where the pairons coherently condense. With this unbinding the electronic entropy recovers to its bare quasiparticle linear-in- $T$  value. We show that this is inconsistent with the measured specific heat which reveals an entropy which never recovers to the highest temperature investigated (about 400 K). In the case of  $\text{Bi}_2\text{Sr}_2\text{CaCu}_2\text{O}_8$  and  $\text{La}_{2-x}\text{Sr}_x\text{CuO}_4$  there is a broad peak above  $T_c$  in the specific heat coefficient,  $\gamma$ , but this arises from the nearby van Hove singularity (vHs) which is more distant in the case of  $\text{Y}_{0.8}\text{Ca}_{0.2}\text{Ba}_2\text{Cu}_3\text{O}_y$  and therefore not discernible. We propose a number of further critical tests. In the pairon model the BCS ratios are not satisfied until vanishingly near where superconductivity disappears in the heavily overdoped region whereas, experimentally, these mean-field ratios are sustained across the overdoped regime once the pseudogap has closed at critical doping.

DOI: [10.1103/PhysRevB.107.054507](https://doi.org/10.1103/PhysRevB.107.054507)

### I. INTRODUCTION

Many aspects of the physics of cuprate high-temperature superconductors (HTS) remain unresolved. This is especially the case in relation to the so-called pseudogap [1–3], a partial gap in the electronic density of states (DOS) observed near the  $(\pi, 0)$  antinodal zone boundary. Researchers cannot agree even on its basic phenomenology, its phase boundaries, and its physical origins [4]. One compelling idea is that the pseudogap arises from incoherent pairing above  $T_c$  [5]. In two recent papers the idea of “pairons” (incoherent bound pairs above  $T_c$ ) is explored in relation to the specific heat [6] and static magnetic susceptibility [7]. The claim is that “the model explains the distinctive features of the entropy and specific heat throughout the temperature-doping phase diagram” and the susceptibility “is consistent with a pseudogap due to hole pairs, or ‘pairons’ above  $T_c$ ” extending across the entire superconducting phase diagram. More recently, Harrison and Chan also explore the idea of a pseudogap arising from uncondensed pairs above  $T_c$  [8].

Here we identify what we have proposed as the truly distinctive features of the cuprate electronic entropy,  $S$ , and show that they are inconsistent with the pseudogap pairon model in a number of key respects. In particular, while the electronic specific heat,  $\gamma T \equiv T \frac{\partial S}{\partial T}$ , contains all the thermodynamic information it somewhat conceals the central subtle features that are more evident in the entropy. From here on we drop the “electronic” descriptor in  $\gamma$  and  $S$  with the understanding that at no point do we consider the lattice or phonon thermodynamic functions. The key features seen in the entropy are (i) the evidence of permanently lost states reflecting a partial gap

in the density of states near the Fermi level (the pseudogap) that never closes at elevated temperature [9], and (ii) the abrupt disappearance of this gap with increasing doping, occurring at a critical doping, independent of temperature [4]. A recent angle-resolved photon electron spectroscopy (ARPES) study confirms this latter view [10].

### II. THERMODYNAMICS IN THE PAIRON MODEL

The pairon model [6] proposes that bound hole pairs form above  $T_c$  due to the local antiferromagnetic environment. This pairing interaction has a binding energy,  $\Delta_p$ , the energy scale of which is governed by  $J$ , the nearest-neighbor exchange interaction. The binding energy in turn sets a characteristic temperature scale,  $T^*$ , around which the pairs unbind. At a low enough temperature the pairs condense into a long-range phase-coherent state and this defines the superconducting  $T_c$ . Local pairing of course lowers the entropy, while coherent condensation lowers the entropy further, beginning abruptly at  $T_c$ . So, qualitatively, from  $T = 0$  we expect  $S(T)$  to rise steadily as quasiparticles excite from the condensate, with a more rapid mean-field-like rise close to  $T_c$  followed by a slower rise above  $T_c$ , followed finally by a further rise near  $T^*$  when the pairons unbind. Above  $T^*$  the entropy,  $S(T)$ , should then follow the roughly linear behavior normally associated with weakly-interacting quasiparticles. Accordingly,  $\gamma(T)$  will show a jump at  $T_c$  characteristic of a second-order phase transition and a hump in the neighborhood of  $T^*$  associated with this eventual unbinding. (Noat *et al.* use the symbol  $T_h$  for this temperature [6]). The jump in  $\gamma(T)$  at  $T_c$  will be diminished due to the pairing correlations above  $T_c$  but with increasing doping, as the pairing above  $T_c$  weakens and  $T^*$  falls, so the jump  $\Delta\gamma_c$  will be less suppressed—it will increase toward the BCS value, reaching that asymptotically as  $T^* \rightarrow 0$ .

\*jeff.tallon@vuw.ac.nz

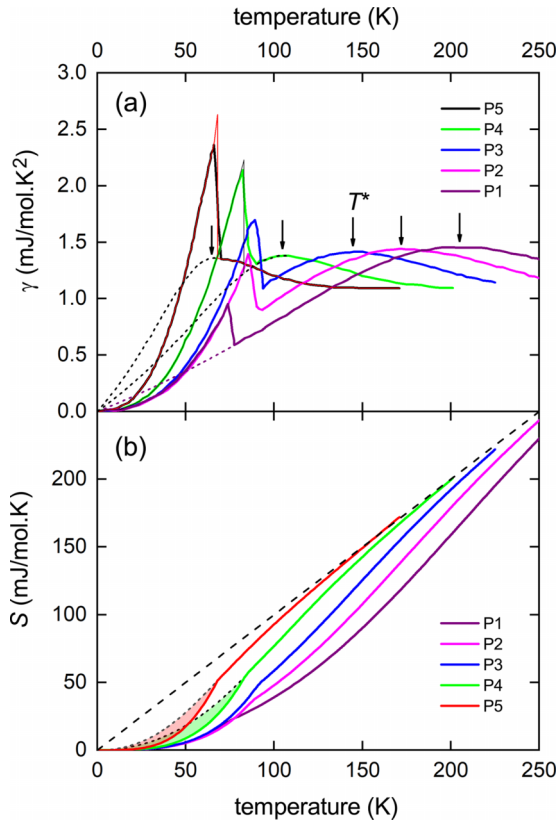


FIG. 1. (a) The electronic specific heat coefficient,  $\gamma$ , calculated by Noat *et al.* [6] under the “pairon” model, and (b) the electronic entropy calculated from  $\gamma$  in (a) by integration. The black short dashed curves are the normal state values if superconductivity is suppressed subject to the constraint of entropy conservation:  $S_n(T_c) = S_s(T_c)$ , where the subscript n refers to the normal state and subscript s refers to the superconducting state. In (b), for the sake of visual clarity, only the normal-state curves are shown for the most overdoped samples P4 and P5. The area between  $S_n(T)$  and  $S_s(T)$  is shown by the shaded region and integrated to obtain the superconducting condensation energy,  $U_0$ .

These expectations are fully borne out by the calculations of Noat *et al.* [6] Fig. 1(a) shows  $\gamma(T)$  calculated under the pairon model for five different doping states spanning the superconducting phase diagram. Figure 1(b) shows the entropy calculated by integrating  $\gamma(T)$  from  $T = 0$ . The key observation is that when the temperature exceeds  $T^*$  the entropy recovers to its noninteracting-quasiparticle value, linear to the origin (see dashed line). This recovery of lost entropy inevitably appears in  $\gamma \equiv \partial S/\partial T$  as a prominent broad peak above the second-order anomaly at  $T_c$ , as highlighted by the arrows in Fig. 1(a). With increasing doping this peak migrates to lower temperature as  $T^*$  falls with doping towards  $T_c$ . In their model  $T^* \rightarrow 0$  as  $T_c \rightarrow 0$  as plotted later in Fig. 3(a) by the olive triangles and thick grey line. This overall behavior is to be compared with the experimentally-observed phenomenology which we now summarize.

### III. ACTUAL CUPRATE THERMODYNAMICS

Different cuprates exhibit some overall generic thermodynamic features but also some variation which arises from the

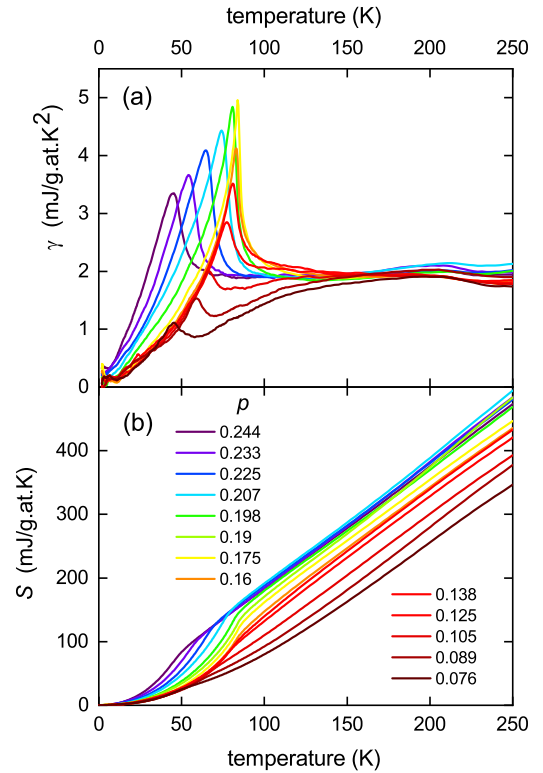


FIG. 2. (a) The measured electronic specific heat coefficient,  $\gamma$ , for  $Y_{0.8}Ca_{0.2}Ba_2Cu_3O_{7-\delta}$  reported by Loram *et al.* [12]; and (b) the electronic entropy calculated from  $\gamma$  in (a) by integration. The doping states span from underdoped  $p \approx 0.07$  to overdoped  $p \approx 0.23$  in small steps of approximately 0.01.

proximity, in some, of the van Hove singularity (vHs). We start with the data for  $Y_{0.8}Ca_{0.2}Ba_2Cu_3O_{7-\delta}$  where the vHs is too far below the Fermi level to be seen in the specific heat [11]. The data is reported by Loram *et al.* [12,13] and is shown in the corresponding  $\gamma(T)$  and  $S(T)$  plots in Figs. 2(a) and 2(b).

Key differences from the calculated behavior are immediately apparent. The entropy can be seen to never recover at higher temperature. There is no evident  $T^*$  location indicating such a recovery. Instead the underdoped entropy curves are displaced downwards in parallel fashion to the highest temperatures studied, in the case of  $YBa_2Cu_4O_8$ , to 400 K [9]. (A similar conclusion has been drawn from the parallel downward displacement of NMR  $1/T_1(T)$  relaxation rates by the group of Haase [14]). As a consequence,  $\gamma(T)$  does not exhibit the anticipated broad peak above  $T_c$ . As noted elsewhere [9], the convergence of  $\gamma(T)$  curves to a single value at high temperature for many different doping levels, combined with a downward parallel displacement of  $S(T)$  curves is indicative of a normal-state gap above  $T_c$  (the pseudogap) which remains open to the highest temperatures. This is incompatible with the pairon model as the pairs are expected to dissociate at elevated temperature leading to the above-noted entropy recovery. Also evident in Fig. 2 is the fact that the downward displacement of  $S(T)$  occurs only in the underdoped and optimally-doped regions. The curves all come together at a critical doping of  $p \approx 0.19$  as extensively discussed previously [4]. This indicates the abrupt closure

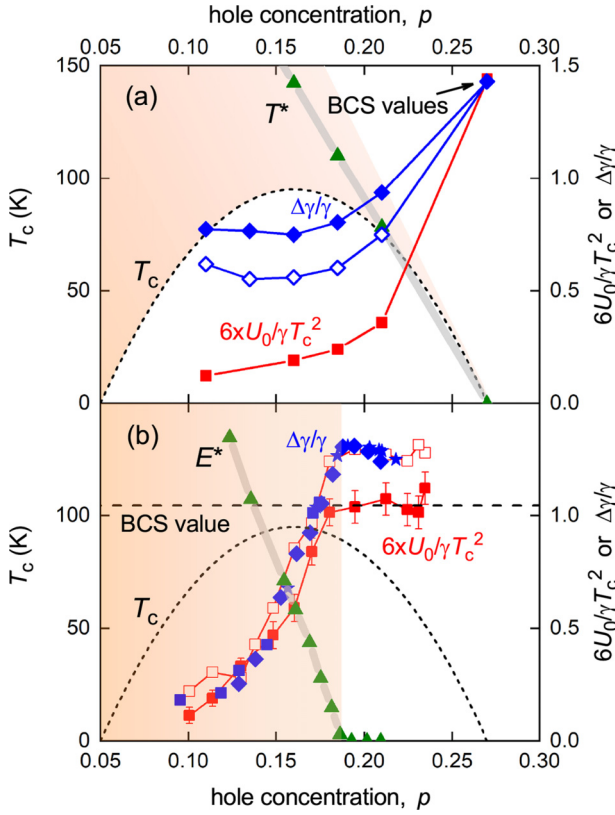


FIG. 3. Comparing (a) pairon and (b) actual experimental scenarios. The respective pseudogap regimes are denoted by orange shading. (a) Red squares:  $U_0/\gamma_c T_c^2$  from integration of the calculated entropy of Noat *et al.* [6]. Blue diamonds: the normalized jump,  $\Delta\gamma/\gamma_c$ , at  $T_c$ . Open blue diamonds: as reported. Full blue diamonds: allowing for abrupt jump in  $\gamma$  subject to entropy conservation. Both ratios fall well below their BCS values 0.24 and 1.43, respectively, due to pairing above  $T_c$ . Olive triangles and gray curve show  $T^*$  values for the hump in  $\gamma(T)$ . At  $p = 0.27$  the limiting ratios reach the BCS values which are plotted at the highest doping. (b) Red open squares:  $U_0/\gamma_c T_c^2$  [12] and filled red squares:  $U_0/\gamma_c T_c^{\text{mf}2}$  [15] for  $\text{Y}_{0.8}\text{Ca}_{0.2}\text{Ba}_2\text{Cu}_3\text{O}_{7-\delta}$ . Blue symbols show  $\Delta\gamma/\gamma_c$  for  $\text{Bi}_2\text{Sr}_2\text{CaCu}_2\text{O}_{8+\delta}$ ; diamonds: pure  $\text{Bi}2212$ ; stars 0.2 Pb doped  $\text{Bi}2212$ ; squares: 0.15 Ca doped  $\text{Bi}2212$ . Experimentally there is no  $T^*$  but values of the pseudogap energy,  $E^*$ , are shown as  $E^*/2.5k_B$  which vanishes at  $p \approx 0.19$ .

of the pseudogap at this critical doping and its complete absence in the overdoped region beyond—as recently confirmed by ARPES measurements [10]. Even if the gap lies asymmetrically below the Fermi level (as in the AF or YSZ reconstruction models near critical doping [16]) it will still be seen in a suppressed linear entropy at high temperature. All these important details, we suggest, are incompatible with the association of the pseudogap with pairons, or any other manifestation of real-space pairs above  $T_c$ .

#### IV. BCS RATIOS

We summarize in Fig. 3 the key differences between the phase behavior and thermodynamic BCS parameters for (a) the pairon scenario, as compared with (b) the experimental data. In (a) the orange shaded area shows the region of

uncondensed pairons, effectively the pseudogap domain under the pairon model. The olive triangles and thick gray line show the values of  $T^*$  descending to zero as  $T_c \rightarrow 0$ , as presumed by Noat *et al.* [6]. In (b) the orange-shaded region shows the experimental pseudogap domain which terminates abruptly at  $p^* = 0.19$  independent of temperature [4,10,13]. While experimentally there is no observable  $T^*$  value at which the pseudogap closes, the pseudogap energy  $E^*$  falls with increasing doping and this is plotted in Fig. 3(b) as  $E^*/2.5k_B$  by the olive triangles and thick gray curve. This falls abruptly to zero at  $p \approx 0.19$ .

We proceed now to compare BCS ratios. While the pairon authors do not explicitly state that their calculations are for  $s$  wave, the low-temperature exponential behavior of  $\gamma(T)$  indicates the  $s$ -wave assumption. For  $d$  wave, the low- $T$  behavior would be linear. In Fig. 1(a) the black short dashed curves are the expected normal-state values of  $\gamma(T)$  if superconductivity is suppressed subject to the constraint of entropy conservation:  $S_n(T_c) = S_s(T_c)$ , where the subscript “n” refers to the normal state and subscript “s” refers to the superconducting state. Two of these dashed curves are omitted for the sake of clarity. In addition, the course graining of calculated data leads to a broadened anomaly at  $T_c$  so we have additionally enforced an abrupt entropy-conserving second-order jump, shown for the two highest doping levels by the thin red and black curves, respectively. By integrating  $\gamma_n(T)$  we obtain  $S_n(T)$  shown by the short dashed curves in Fig. 1(b). And then by integrating  $\Delta S(T) = S_n(T) - S_s(T)$  we obtain the condensation energy  $U_0 = U(T = 0)$ . This is the pink or green shaded area under the short dashed curves in Fig. 1(b). Within the Bardeen, Cooper, and Schrieffer (BCS) theory, the ratio  $U_0/\gamma_c T_c^2$  should be a constant with the value 0.24 for the  $s$ -wave superconductivity assumed by Noat *et al.* [6]. This ratio is plotted as a function of doping by the red squares in Fig. 3(a) and we multiply by  $6\times$  to scale conveniently with  $\Delta\gamma/\gamma_c$ . The open blue diamonds show values of  $\Delta\gamma/\gamma_c$  taken directly from the curves of Noat *et al.*, while the solid blue diamonds show values of  $\Delta\gamma_c/\gamma$  when an abrupt transition is enforced at  $T_c$ .

All ratios are seen to fall well below the canonical BCS values and this is due to the parapaing that occurs above  $T_c$ . Enforcing an abrupt jump at  $T_c$  (filled diamonds) leads to higher values of  $\Delta\gamma_c/\gamma$  but they still remain far short of the BCS value of 1.43. Under the assumptions of Noat *et al.* this parapaing vanishes at  $p = 0.27$  where  $T^* \rightarrow 0$  (and superconductivity disappears) and so the limiting values of  $U_0/\gamma_c T_c^2$  and  $\Delta\gamma_c/\gamma$  must reach the BCS values there. We therefore plot these limiting BCS values at  $p = 0.27$ , shown by the terminal squares and diamonds. The overall trend is obvious—that of steadily increasing ratios as  $T^*$  falls with doping. Moreover, the model has no discontinuity that would cause any abrupt departure from a smooth and steady rise toward those BCS values. These curves are expected to be featureless across the superconducting phase diagram.

In contrast, the experimental data shown in Fig. 3(b) reveal an abrupt change occurring near  $p = 0.19$  where the pseudogap closes. Values for  $U_0/\gamma_c T_c^2$  are shown for  $\text{Y}_{0.8}\text{Ca}_{0.2}\text{Ba}_2\text{Cu}_3\text{O}_{7-\delta}$  reported by Loram *et al.* [13] (open red squares). On the overdoped side ( $p > 0.19$ ) the data is more or less constant around 0.21, then fall abruptly when

$p$  drops below 0.19 and the pseudogap opens. The mean-field BCS ratio for  $d$ -wave superconductivity is 0.174. However, strong fluctuations in the cuprates result in a substantial depression of  $T_c$  below the mean-field value,  $T_c^{\text{mf}}$ , which can be deduced from an entropy-conserving fluctuation analysis [17]. The solid red squares show the resultant values of  $U_0/\gamma_c T_c^{\text{mf}^2}$  and these indeed sit close to the weak-coupling  $d$ -wave BCS ratio shown by the horizontal dashed line. We conclude that, in the overdoped region ( $p > 0.19$ ), the pseudogap is absent and that the superconductivity is conventional in the sense that the BCS condensation energy ratio is conserved. Then, rather abruptly at  $p \approx 0.19$ , this ratio falls with the opening of the pseudogap, unlike the pairon model where the ‘‘pseudogap’’ remains open to the very end of the superconducting phase diagram.

Turning to the ratio  $\Delta\gamma/\gamma_c$ , a similar result is found for  $\text{Y}_{0.8}\text{Ca}_{0.2}\text{Ba}_2\text{Cu}_3\text{O}_{7-\delta}$  [12] and also for  $\text{Bi}_2\text{Sr}_2\text{CaCu}_2\text{O}_{8+\delta}$ . Figure 3(b) shows  $\Delta\gamma/\gamma_c$  for the latter compound (blue data points). There are three different samples represented here: blue diamonds are for the pure compound, blue stars for 0.2 Pb doped Bi2212 (which allows a higher doping range) and blue squares for 0.15 Y doped on the calcium site (which allows a lower doping range). The three data sets are all consistent showing a plateau down to  $p \approx 0.19$  followed by a rapid collapse for  $p < 0.19$ , again reflecting the opening of the pseudogap. The values on this plateau are around 1.25 while the weak-coupling BCS ratio is  $\Delta\gamma/\gamma_c = 0.955$ . But again, the presence of strong superconducting fluctuations in the neighborhood of  $T_c$  result in an additional fluctuation contribution to  $\Delta\gamma$  (as well as the marked reduction in  $T_c$ ). This has been analyzed in detail using the above-noted fluctuation analysis [17]. For Bi2212 the mean-field jump,  $\Delta C_p$ , in specific heat at  $p = 0.19$  is  $120.2 \pm 10$  mJ/(g at K),  $T_c^{\text{mf}}$  is 124.6 K, while the background normal-state  $\gamma$  is 1.05 mJ/(g at K<sup>2</sup>), giving a mean-field ratio,  $\Delta\gamma^{\text{mf}}/\gamma_c$ , of  $0.92 \pm 0.07$ , rather close to the weak-coupling BCS value. We note finally that the raw jump in specific heat coefficient is the most accurately determined feature of these differential specific heat measurements and it provides rather clear evidence that the pseudogap is absent for  $p > 0.19$  and opens abruptly as doping falls below this threshold.

As a consequence, the pseudogap  $T^*(p)$  line cannot extend across the entire superconducting phase curve as shown by the green diamonds and gray curve in Fig. 3(a). Though widely embraced, this idea is largely referenced to Vishik *et al.* [18], and this group no longer subscribes to this view [10]. In the original source data (Fig. 4(f) of Ref. [18]) the  $T^*$  values are not temperatures at all but antinodal energy gaps converted to a temperature scale merely by dividing by Boltzmann’s constant,  $k_B$ . As such they reflect the (larger) pseudogap in the underdoped region and the superconducting gap in the overdoped region where the pseudogap is absent [10]. Naturally, the superconducting gap vanishes along with  $T_c$ , but this has no bearing on the pseudogap or its crossover boundary at  $T^*$ . This issue is discussed in detail elsewhere [4].

## V. SUPERFLUID DENSITY

The above arguments do not of course discount the presence of pairons above  $T_c$ , they simply question the

identification of pairons with the pseudogap. We have already noted the strong superconducting fluctuations present above  $T_c$  and extending up to around  $T_c^{\text{mf}}$  which, in the case of  $\text{Y}_{0.8}\text{Ca}_{0.2}\text{Ba}_2\text{Cu}_3\text{O}_{7-\delta}$ , lies up to 30 K above  $T_c$  and up to 45 K above  $T_c$  in the case of Bi2212 [17] near optimal doping. This persistent parapairing is equivalent to the presence of pairons in a somewhat narrow crescent band above  $T_c$  extending across the phase diagram. We have previously mapped this in detail [17] and more recently the phase extent of these fluctuations and the associated pairing gap have been confirmed in ARPES measurements [10,19].

Consistent with these ARPES measurements, the pairon temperature scale will follow a roughly dome-shaped curve lying above the  $T_c(p)$  phase curve defining a crescent of pairing fluctuations above  $T_c$ . It is most likely defined by the temperature scales for phase,  $T_\theta$ , and amplitude,  $T_{\text{amp}}$ , fluctuations. Elsewhere [17] it was shown that, for cuprates, these two temperature scales are essentially equal, given by

$$k_B T_{\text{amp}} \approx k_B T_\theta = \frac{0.9d\hbar^2}{4\mu_0 e^2} \times \lambda_{ab}^{-2}, \quad (1)$$

where  $d$  is the mean interlayer spacing,  $\lambda_{ab}$  is the in-plane London penetration depth, and  $\lambda_{ab}^{-2}$  is often referred to loosely as the superfluid density,  $\rho_s$ . Its doping dependence indeed follows a dome, collapsing on both the underdoped and overdoped sides [20,21].

This relatively narrow crescent of fluctuations above  $T_c$  must be distinguished from the pseudogap which exists to very high temperature and which, according to thermodynamic [12,13,17] and optical measurements [22], coexists with superconductivity down to the groundstate at  $T = 0$ , as depicted by the orange shaded area in Fig. 3(b). For a brief discussion on whether the pseudogap competes with superconductivity, or merely coexists, see Supplemental Material (SM) [23] (see also, Refs. [24–28] therein). In view of this coexistence we make the following prediction. If the ground-state superfluid density is calculated within the pairon model it will be featureless across the superconducting phase diagram. This is because all pairons have condensed at  $T = 0$ . Stated another way, the supposed pseudogap arising from parapairing above  $T_c$  should be absent at  $T = 0$ , as emphasized by the orange shaded area in Fig. 3(a). Contrasting this, the experimentally-observed ground-state superfluid density exhibits an abrupt discontinuity at  $p \approx 0.19$ , falling away sharply below this doping due to the abrupt opening of the pseudogap [21]. The pseudogap is present in the ground state at  $T = 0$  and this is the foremost objection to those models [6,8] which identify the pseudogap with pairing above  $T_c$ .

There are thus at least four central features of the thermodynamic parameters of cuprates which argue against the pairon model. First, the ‘‘lost entropy’’ associated with the pseudogap never recovers at high temperature. Second, the relative jump in  $\gamma$  at  $T_c$  begins to collapse abruptly when  $p$  falls below 0.19 due to the abrupt opening of the pseudogap. This is a signature of the abrupt depletion of condensed pairs and is seen in  $\text{Y}_{0.8}\text{Ca}_{0.2}\text{Ba}_2\text{Cu}_3\text{O}_{7-\delta}$ ,  $\text{Bi}_2\text{Sr}_2\text{CaCu}_2\text{O}_{8+\delta}$ , and  $\text{La}_{2-x}\text{Sr}_x\text{CuO}_4$  and is presumed to be universal. Third, there is a collapse in the BCS-scaled condensation energy when  $p$  falls below 0.19. This also appears to be more or less

universal. Fourth, the ground-state superfluid density likewise shows a universal abrupt collapse at the same doping point, whereas it is expected to be featureless in the pairon model.

## VI. VAN HOVE SINGULARITY

The “lost entropy” phenomenology and its abrupt termination at critical doping is clear in the case of  $Y_{0.8}Ca_{0.2}Ba_2Cu_3O_{7-\delta}$  but is perhaps more subtle for  $Bi_2Sr_2CaCu_2O_{8+\delta}$  and  $La_{2-x}Sr_xCuO_4$ . This is due to the proximity of the van Hove singularity (vHs) in the latter compounds [29–31], unlike  $YBa_2Cu_3O_{7-\delta}$  and  $Y_{0.8}Ca_{0.2}Ba_2Cu_3O_{7-\delta}$  where the vHs lies beyond the superconducting dome [11]. The approach to the vHs causes an upward displacement of the linear high-temperature entropy curves which could be confused with that found as the pseudogap closes, if the two features lie close to each other. This may not be all that unlikely. The vHs probably defines the upper limit for  $p^*$  because the pseudogap is located on the zone-boundary antinodal states which are absent on the electron-like Fermi surface beyond the vHs. There is some experimental [32] and theoretical [33] evidence that  $p^*$  may lie at the vHs, or just below it [34]. However, the thermodynamic data does not support this and we will see that  $p^*$  lies safely below  $p_{vHs}$  for  $La_{2-x}Sr_xCuO_4$  (La214) and for  $Bi_2Sr_2CaCu_2O_{8+\delta}$  (Bi2212).

As discussed in Ref. [9] the entropy for weakly-interacting electrons is given by an integral of the density of states weighted by a Fermi window which is peaked at the Fermi level—see Eq. (2) below. Increasing temperature broadens the window but it remains peaked at  $E_F$ . Thus, if there exists a normal-state gap near  $E_F$ , which does not close with increasing temperature, then this Fermi window will always see the gap even at the highest temperature and the entropy is accordingly displaced downwards (with a linear intercept directly proportional to the gap magnitude).

In contrast,  $\gamma(T)$  is the  $T$  derivative of  $S(T)$  and so its Fermi window is a double peaked function with peaks either side of the Fermi level. At high enough temperature these peaks will shift outside the gap, the gap will not be seen in the integral, and so  $\gamma(T)$  recovers to its background weakly-interacting-Fermion value. This is precisely what is seen in Figs. 2(b) and 2(a), respectively, for  $Y_{0.8}Ca_{0.2}Ba_2Cu_3O_{7-\delta}$ .

But importantly, the same argument applies if there is a peak near  $E_F$  in the electronic DOS—such as that arising from a vHs. In this case  $S(T)$  at high  $T$  will be displaced upwards in parallel fashion while  $\gamma(T)$  merely returns to its background value after passing through a hump located at  $T \approx \Delta E_{vHs}/4k_B$ , where  $\Delta E_{vHs}$  is the location of the vHs relative to  $E_F$ . Clearly then, the proximity of the vHs in the lightly overdoped region confuses the interpretation of the high temperature-entropy because  $S(T)$  no longer saturates at critical doping but continues to shift upwards beyond  $p^*$ . On approaching the vHs  $S(T)$  will continue shifting upwards reaching a maximum when the vHs crosses  $E_F$  before shifting down again on the other side of the vHs. While there is a pseudogap present, the effect of the vHs will be somewhat concealed in the antinodal gap. It will only emerge, if sufficiently close to the Fermi surface, when the pseudogap closes, or is about to close.

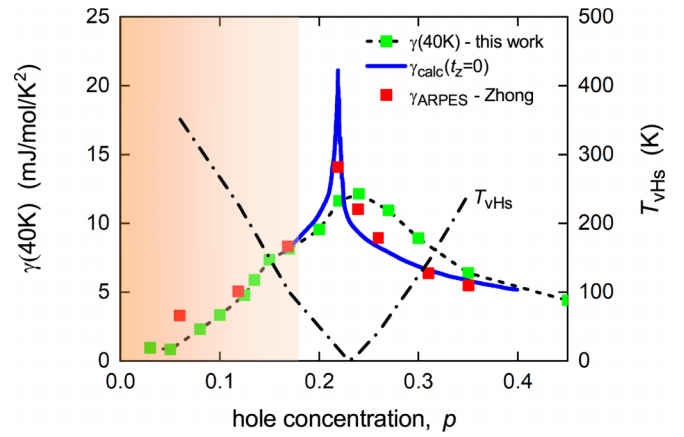


FIG. 4. Normal-state experimental values of  $\gamma(40\text{ K})$ , read off from Fig. S.1, plotted as a function of doping for  $La_{2-x}Sr_xCuO_4$  (green squares). These are compared with  $\gamma(2\text{ K})$  calculated by Zhong *et al.* [36] from the ARPES 3D dispersion (red squares) and assuming a zero interlayer hopping parameter,  $t_z$ , i.e., 2D (blue curve). Apart from the location of the vHs there is excellent agreement between the experimental and calculated data. The orange shaded area shows the extent of the pseudogap. The black dash dot curve shows the doping evolution of  $T_{vHs}(p)$  obtained by calculating  $\chi_s(T)$  from the tight-binding dispersion fits by Zhong *et al.* [36] using Eq. (3).

All these features are seen in the experimental data for La214 and Bi2212 as originally reported by Loram *et al.* [12]. The relevant figures are reproduced in the SM in Figs. S.1 and S.2, respectively. For the sake of clarity, in the case of Bi2212 we do not show the original data points, just the normal-state fits to the data [35]. These fits are calculated using a rigid ARPES-derived anti-bonding-band dispersion reported by Kaminski *et al.* [29] using the standard noninteracting model for calculating the entropy [see Eq. (2) below] with the additional requirement of entropy conservation relative to the experimental data. The legend shows the doping states for each curve and the corresponding values of  $\Delta E_{vHs}$  obtained from the fits [35].

While, for both La214 and Bi2212, the opening of the pseudogap is apparent from the sudden collapse of  $\Delta\gamma/\gamma$ , it is much harder to pin down from the parallel shift of  $S(T)$  curves. This shift is now associated with both the pseudogap and the approach to the nearby vHs. In the entropy it is really only indicated by the observation that  $S(T)$  is linear to the origin at  $p \approx 0.19$ . The local peak in  $\gamma(T)$  arising from the vHs [see arrows in Figs. S.1(a) and S.2(a)] is seen to migrate towards  $T = 0$  as  $\Delta E_{vHs} \rightarrow 0$  then shift up in temperature again once the Fermi surface becomes electronlike. It is this vHs-derived peak in  $\gamma(T)$  which Noat *et al.* possibly confuse with their anticipated peak in  $\gamma(T)$  arising from the depairing of pairons and shown in Fig. 1(a)—especially at higher dopings where the vHs peak is more prominent. But the phenomenology is quite different. At the same doping both the  $\gamma(T)$  and  $S(T)$  curves rise to a maximum height then fall again on crossing the vHs. The experimental values of  $\gamma(40\text{ K})$  for La214 taken from Fig. S.1 are plotted in Fig. 4 as a function of doping (green squares). They rise to a peak at  $x \approx 0.23$ . This is essentially consistent with

recent ARPES measurements by Zhong *et al.* of the doping-dependent 3D dispersion, from which  $\gamma(T)$  was calculated [36]. Values of  $\gamma(2\text{ K})$  from these calculations are plotted in Fig. 4 (red squares). In addition, the figure shows the specific heat coefficient,  $\gamma(2\text{ K})$ , calculated by these authors when the interlayer hopping parameter  $t_z$  is zero i.e., the 2D case (blue curve). These ARPES measurements and calculation of  $\gamma(T)$  by Zhong *et al.* resolved an earlier reported discrepancy in calculated  $\gamma(T)$  [37] by adopting doping-dependent hopping parameters  $t_2$  and  $t_3$  and by carrying out the full calculation of  $\gamma(T) = \partial S/\partial T$  using Eq. (2) below.

The measurements of Zhong *et al.* locate the crossing point, and the associated peak in  $\gamma(T)$ , at 0.21 [36], but otherwise are in excellent quantitative agreement with our experimental data. (We are restricted to 40 K for this data because of the intervention of superconductivity at lower temperatures. The peak in  $\gamma(p, T)$  will be sharper at lower temperature.) It is clear from a comparison of the ARPES-derived  $\gamma(T)$  with the experimental data that the peak in  $\gamma(T)$  is attributable solely to the vHs and the only disparity is in the location of the crossing point,  $x = 0.21$ , in the ARPES experiments and  $x = 0.23$  in the bulk specific heat measurements. We note that the ARPES measurements were on thin films and perhaps the slightly lower doping state for the vHs crossing, compared with bulk samples, is attributable to epitaxial stress in the former.

For Bi2212 (see Fig. S.2) the vHs is projected to cross the Fermi surface at  $p = 0.225$ , consistent with Kaminski *et al.* [29]. [Though this is much the same crossing point as was found for La214 we consider this coincidental. Indeed, two recent studies [38,39] show that at  $p \approx 0.23$  the vHs still lies below the Fermi level. For our purpose the precise location is not too important but we do note that the specific heat studies are more consistent with Kaminski.] For each doping level the peaks in  $\gamma(T)$ , arising from the vHs, are again annotated by arrows and their progression toward  $T = 0$  at the vHs is clearly evident. They occur at  $T \approx \Delta E_{\text{vHs}}/4k_B$ , and on crossing the vHs these peaks move up in temperature again. (Such a band-structure-derived peak in  $\gamma(T)$  can be seen e.g., in  $\text{Sr}_3\text{Ru}_2\text{O}_7$  [40]). Notice once more how all the  $\gamma(T)$  curves converge to a single value at high temperature, while the  $S(T)$  curves spread out in parallel fashion to the highest temperature without converging. Curves are linear to the origin only when  $0.18 < p < 0.19$ , the location of critical doping where the pseudogap vanishes, and the point at which  $\Delta\gamma/\gamma$  suddenly collapses. We stress the very different behavior seen in Figs. S.1 and S.2 from that shown in Fig. 1 for the pairon model. This dominating presence of the vHs in Bi2212 and La214 is relevant also to the interpretation of the spin susceptibility, to which we now turn.

## VII. SPIN SUSCEPTIBILITY

In their second paper Noat *et al.* [7] turn their attention to interpreting the static magnetic susceptibility within their pairon model. The spin susceptibility and electronic entropy are closely related, both representing similar weighted integrals of the electronic density of states. As a consequence each of the points raised above is also relevant to the spin susceptibility. To see this consider the entropy for a weakly-interacting

Fermi liquid [41]:

$$S_n = -2k_B \int_{-\infty}^{\infty} [f \ln(f) + (1-f) \ln(1-f)] N(E) dE, \quad (2)$$

where  $f(E)$  is the Fermi function and  $N(E)$  is the electronic DOS for one spin direction. This is just a weighted integral of the DOS with the ‘‘Fermi window’’  $[f \ln(f) + (1-f) \ln(1-f)]$ .

On the other hand, the spin susceptibility for a weakly-interacting Fermion system is

$$\chi_s = -2\mu_B^2 \int_{-\infty}^{\infty} \frac{\partial f(E)}{\partial E} N(E) dE. \quad (3)$$

The susceptibility is an integral of the DOS where the Fermi window is now the function  $\partial f/\partial E$ . It turns out that  $T \partial f/\partial E$  is essentially identical to  $[f \ln(f) + (1-f) \ln(1-f)]$  if  $\chi_s$  in the former is stretched in temperature by a factor 1.187 [42]. Therefore,  $S/T$  and  $\chi_s$  are closely related. This relationship is often expressed by the Wilson ratio,  $a_W$ , such that  $S(T)/T = a_W \chi_s(T)$ , where

$$a_W = \frac{1}{3\mu_0} \left( \frac{\pi k_B^2}{\mu_B} \right)^2. \quad (4)$$

A number of studies have shown that this relationship is sustained in the cuprates across a broad range of temperatures and doping [9,13,42,43]. Noat *et al.* [7] fit the experimental static susceptibility data for La214, Bi2212, and Y123 using a four-term model comprising a constant term (representing the atomic core and Van Vleck terms), an antiferromagnetic term,  $\chi_{\text{AF}}$ , a Pauli term (arising from the delocalized electrons), and a diamagnetic term (arising from circulating supercurrents near  $T_c$ ). The third, Pauli, term is essentially the spin susceptibility given by Eq. (3) which we have shown is entirely consistent with the presence of a temperature-independent normal-state gap which does not close at elevated temperature. Accordingly, it is incompatible with a pairon gap which evaporates around  $T^*$ . The second term,  $\chi_{\text{AF}}$ , is modeled as

$$\chi_{\text{AF}}(T) = A_{\text{mag}} \left( T + \frac{T_{\text{max}}^2}{T} + C \right)^{-1}. \quad (5)$$

This has a peak at  $T_{\text{max}}$  reflecting a characteristic underlying energy scale associated with antiferromagnetic correlations. By omitting the vHs in the Pauli term, the fits naturally attempt to vest the vHs peak in  $\chi_s$  with the  $\chi_{\text{AF}}$  term. Whereas  $T_{\text{max}}$ , associated with  $\chi_{\text{AF}}$ , should decrease monotonically as the AF correlations weaken, the vHs-derived peak in  $\chi_s(T)$  (located at  $T_{\text{vHs}}$ ) moves down to  $T = 0$  at the vHs crossing and then rises again to increasingly elevated temperatures as the Fermi level moves beyond the vHs [36,44]. We have calculated  $\chi_s(T)$  from the tight binding fits of Zhong *et al.* [36] using Eq. (3) and measured the position,  $T_{\text{vHs}}$ , of the local peak in  $\chi_s(T)$ . The doping dependence of  $T_{\text{vHs}}(p)$  is shown in Fig. 4 by the dash dot curve. Its nonmonotonic V-shaped character, centered on the vHs, is evident. Neglecting the vHs will thus result in an inferred  $T_{\text{max}}(p)$  which falls to zero at the vHs then rises again. This can possibly be seen in the data fits of Noat *et al.* [7] where  $T_{\text{max}}$  falls linearly with  $p$  extrapolating to zero at  $p \approx 0.23$  (precisely the location of the vHs in our data) but then saturating. The authors have just one data point

beyond  $p = 0.23$  thus giving the appearance of a saturation in  $T_{\max}(p)$ , but our interpretation would suggest that pushing out to higher doping will reveal a V-shaped  $p$  dependence of the deduced  $T_{\max}(p)$  arising from the vHs, rather than an ongoing monotonic decrease due to weakening of AF correlations.

Finally, we note that within the pairon model  $\chi_s(T)$  near a vHs will possess a broad peak analogous to that in  $\gamma(T)$ . And if we construct  $T\chi_s(T)$ , the analog of  $S(T)$ , this should recover to the background quasiparticle value at high temperature. It does not. Rather,  $T\chi_s(T)$ , like  $S(T)$ , exhibits a set of parallel lines at high temperature displaced downwards by the pseudogap and showing no sign of recovery to at least 400 K—see Fig. 13(a) of Ref. [13] or to at least 550 K in the measurements of Nakano *et al.* [45].

### VIII. CONCLUSIONS

In summary, we have made six key points:

(i) while the pairon model requires the entropy to recover at some elevated temperature ( $T^*$ ) where the pairons dissociate, no such recovery is observed in the experimental data to the highest investigated temperature, at least to 400 K [4,9]. The pseudogap remains open to a very high temperature scale, provided that  $p < 0.19$ .

(ii) The experimental data fails to show any peak in  $\gamma(T)$  associated with such an entropy recovery. However, there is for some overdoped cuprates an increasingly prominent peak associated with traversing the proximate van Hove singularity.

(iii) In the pairon model the BCS ratios  $\Delta\gamma/\gamma_c$  and  $U_0/\gamma_c T_c^2$  are suppressed well below the canonical BCS values across the entire superconducting phase diagram due to the presence of pairons above  $T_c$  throughout. In contrast, the experimental data shows that these ratios remain more or less constant for  $p > 0.19$  but collapse rapidly for  $p < 0.19$  as the pseudogap opens. When scaled with mean-field values (as they should) the ratios are close to the canonical BCS values when  $p > 0.19$ .

(iv) The idea that the pseudogap persists across the entire superconducting phase curve, including the overdoped

region, finds no support in the thermodynamic data shown in Fig. 3(b), nor in recent ARPES data [10]. The pseudogap is present for all  $p < 0.19$ , even in the  $T = 0$  ground state, and is absent for all  $p > 0.19$ , independent of temperature. The boundary is abrupt [4,10].

(v) We predict that, within the pairon model, the  $T = 0$  superfluid density will be featureless as a function of doping, contrasting the experimental observation that  $\lambda^{-2}(p, 0)$  collapses abruptly due to opening of the pseudogap as  $p$  falls below  $p^* = 0.19$ .

(vi) The spin susceptibility,  $\chi_s(T)$ , for  $\text{La}_{2-x}\text{Sr}_x\text{CuO}_4$  and  $\text{Bi}_2\text{Sr}_2\text{CaCu}_2\text{O}_{8+\delta}$  exhibits a peak arising from the nearby van Hove singularity which moves down in temperature as the vHs is approached then is projected to rise again. In all likelihood this is the peak observed by Noat *et al.* [7] and attributed by them to AF correlations. The high-temperature product  $T\chi_s(T)$ , like the entropy  $S(T)$ , exhibits a downward progression of parallel lines with decreasing doping as the pseudogap opens and grows. Contrary to the pairon model,  $T\chi_s(T)$  never recovers its lost weight at high temperature up to at least 550 K, even for dopings close to  $p^*$  where  $E^*$  is small.

We conclude that the pseudogap does not originate in pairon formation but is a distinct state that competes with pairing down to  $T = 0$ . Pairing occurs on the Fermi arcs (or pockets) lying between the pseudogapped antinodes and leads to a downshift in spectral weight below the pairing gap [46]. The pseudogap, confined to the antinodes, results in transfer of spectral weight above the gap [22]. Beyond critical doping,  $p^* = 0.19$ , the pairing  $d$ -wave gap extends over the full Fermi surface.

### ACKNOWLEDGMENTS

We thank John R. Cooper, Cambridge University, for ongoing discussion and critique on the issues discussed herein, and express our continuing debt of gratitude to the late John W. Loram who carried out the thermodynamic measurements reported here.

- 
- [1] M. R. Norman, D. Pines, and C. Kallin, The pseudogap: Friend or foe of high- $T_c$ , *Adv. Phys.* **54**, 715 (2005).
- [2] T. Timusk and B. Statt, The pseudogap in high-temperature superconductors: An experimental survey, *Rep. Prog. Phys.* **62**, 61 (1999).
- [3] J. L. Tallon and J. W. Loram, The doping dependence of  $T^*$ —what is the real high- $T_c$  phase diagram? *Physica C* **349**, 53 (2001).
- [4] J. L. Tallon, J. G. Storey, J. R. Cooper, and J. W. Loram, Locating the pseudogap closing point in cuprate superconductors: Absence of entrant or reentrant behavior, *Phys. Rev. B* **101**, 174512 (2020).
- [5] V. Emery and S. A. Kivelson, Importance of phase fluctuations in superconductors with small superfluid density, *Nature (London)* **374**, 434 (1995).
- [6] Y. Noat, A. Mauger, M. Nohara, H. Eisaki, and W. Sacks, How ‘pairons’ are revealed in the electronic specific heat of cuprates, *Solid State Commun.* **323**, 114109 (2021).
- [7] Y. Noat, A. Mauger, M. Nohara, H. Eisaki, S. Ishida, and W. Sacks, Cuprates phase diagram deduced from magnetic susceptibility: What is the ‘true’ pseudogap line? *Solid State Commun.* **348-349**, 114689 (2022).
- [8] N. Harrison and M. K. Chan, Magic Gap Ratio for Optimally Robust Fermionic Condensation and Its Implications for High- $T_c$  Superconductivity, *Phys. Rev. Lett.* **129**, 017001 (2022).
- [9] J. L. Tallon and J. W. Loram, Field-dependent specific heat of the canonical underdoped cuprate superconductor  $\text{YBa}_2\text{Cu}_3\text{O}_8$ , *Sci. Rep.* **10**, 22288 (2020).
- [10] S.-D. Chen, M. Hashimoto, Y. He, D. Song, K.-J. Xu, J.-F. He, T. P. Devereaux, H. Eisaki, D.-H. Lu, J. Zaanen, and Z.-X. Shen, Incoherent strange metal sharply bounded by a critical doping in  $\text{Bi2212}$ , *Science* **366**, 1099 (2019).
- [11] M. A. Hossain *et al.*, In situ doping control of the surface of high-temperature superconductors, *Nat. Phys.* **4**, 527 (2008).
- [12] J. W. Loram, K. A. Mirza, J. R. Cooper, and J. L. Tallon, Superconducting and normal-state energy gaps in

- $Y_{0.8}Ca_{0.2}Ba_2Cu_3O_{7-\delta}$  from the electronic specific heat, *Physica C* **282-287**, 1405 (1997).
- [13] J. W. Loram, J. L. Luo, J. R. Cooper, W. Y. Liang, and J. L. Tallon, Evidence on the pseudogap and condensate from the electronic specific heat, *J. Phys. Chem. Solids* **62**, 59 (2001).
- [14] J. Nachtigal, M. Avramovska, A. Erb, D. Pavicevic, R. Guehne, and J. Haase, Temperature independent cuprate pseudogap from planar oxygen NMR, *Condens. Matter* **5**, 66 (2020).
- [15] J. L. Tallon, F. Barber, J. G. Storey, and J. W. Loram, Coexistence of the superconducting energy gap and pseudogap above and below the transition temperature of cuprate superconductors, *Phys. Rev. B* **87**, 140508(R) (2013).
- [16] J. G. Storey, Hall effect and Fermi surface reconstruction via electron pockets in the high- $T_c$  cuprates, *Europhys. Lett.* **113**, 27003 (2016).
- [17] J. L. Tallon, J. G. Storey, and J. W. Loram, Fluctuations and critical temperature reduction in cuprate superconductors, *Phys. Rev. B* **83**, 092502 (2011).
- [18] I. M. Vishik *et al.*, Phase competition in trisected superconducting dome, *Proc. Natl. Acad. Sci. USA* **109**, 18332 (2012).
- [19] T. Kondo, W. Malaeb, Y. Ishida, T. Sasagawa, H. Sakamoto, T. Takeuchi, T. Tohyama, and S. Shin, Point nodes persisting far beyond  $T_c$  in Bi2212, *Nat. Commun.* **6**, 7699 (2015).
- [20] Ch. Niedermayer, C. Bernhard, U. Binninger, H. Gluckler, J. Tallon, E. J. Ansaldo, and J. I. Budnick, Muon Spin Rotation Study of the Correlation Between  $T_c$  and  $n_s/m^*$  in Overdoped  $Tl_2Ba_2CuO_6$ , *Phys. Rev. Lett.* **71**, 1764 (1993).
- [21] C. Bernhard, J. L. Tallon, Th. Blasius, A. Golnik, and Ch. Niedermayer, Anomalous Peak in the Superconducting Condensate Density of Cuprate High- $T_c$  Superconductors at a Unique Doping State, *Phys. Rev. Lett.* **86**, 1614 (2001).
- [22] L. Yu, D. Munzar, A. V. Boris, P. Yordanov, J. Chaloupka, Th. Wolf, C. T. Lin, B. Keimer, and C. Bernhard, Evidence for Two Separate Energy Gaps in Underdoped High-Temperature Cuprate Superconductors from Broadband Infrared Ellipsometry, *Phys. Rev. Lett.* **100**, 177004 (2008).
- [23] See Supplemental Material at <http://link.aps.org/supplemental/10.1103/PhysRevB.107.054507> for  $\gamma(T)$  and  $S/T$  for La214 and Bi2212 and also a brief discussion as to whether the pseudogap competes or coexists with superconductivity.
- [24] J. W. Loram, K. A. Mirza, J. R. Cooper, W. Y. Liang, and J. M. Wade, Electronic specific heat of  $YBa_2Cu_3O_{6+x}$  from 1.8 to 300 K, *J. Supercond.* **7**, 243 (1994).
- [25] T. Kondo, R. Khasanov, T. Takeuchi, J. Schmalian, and A. Kaminski, Competition between the pseudogap and superconductivity in the high- $T_c$  copper oxides, *Nature (London)* **457**, 296 (2009).
- [26] J. Kuspert, R. CohnWagner, C. Lin, K. vonArx, Q. Wang, K. Kramer, W. R. Pudelko, N. C. Plumb, C. E. Matt, C. G. Fatuzzo, D. Sutter, Y. Sassa, J. Q. Yan, J. S. Zhou, J. B. Goodenough, S. Pyon, T. Takayama, H. Takagi, T. Kurosawa, N. Momono, M. Oda, M. Hoesch, C. Cacho, T. K. Kim, M. Horio, and J. Chang, Pseudogap suppression by competition with superconductivity in La-based cuprates, *Phys. Rev. Res.* **4**, 043015 (2022).
- [27] T. L. Miller, W. Zhang, H. Eisaki, and A. Lanzara, Particle-Hole Asymmetry in the Cuprate Pseudogap Measured with Time-Resolved Spectroscopy, *Phys. Rev. Lett.* **118**, 097001 (2017).
- [28] J. G. Storey, J. L. Tallon, and G. V. M. Williams, Electron pockets and pseudogap asymmetry observed in the thermopower of underdoped cuprates, *Europhys. Lett.* **102**, 37006 (2013).
- [29] A. Kaminski, S. Rosenkranz, H. M. Fretwell, M. R. Norman, M. Randeria, J. C. Campuzano, J. M. Park, Z. Z. Li, and H. Raffy, The change of Fermi surface topology in  $Bi_2Sr_2CaCu_2O_{8+\delta}$  with doping, *Phys. Rev. B* **73**, 174511 (2006).
- [30] T. Yoshida, X. J. Zhou, K. Tanaka, W. L. Yang, Z. Hussain, Z.-X. Shen, A. Fujimori, S. Sahrakorpi, M. Lindroos, R. S. Markiewicz, A. Bansil, S. Komiyama, Y. Ando, H. Eisaki, T. Kakeshita, and S. Uchida, Systematic doping evolution of the underlying Fermi surface of  $La_{2-x}Sr_xCuO_4$ , *Phys. Rev. B* **74**, 224510 (2006).
- [31] E. Razzoli *et al.*, The Fermi surface and band folding in  $La_{2-x}Sr_xCuO_4$ , probed by angle-resolved photoemission, *New J. Phys.* **12**, 125003 (2010).
- [32] S. Benhabib, A. Sacuto, M. Civelli, I. Paul, M. Cazayous, Y. Gallais, M.-A. Méasson, R. D. Zhong, J. Schneeloch, G. D. Gu, D. Colson, and A. Forget, Collapse of the Pseudogap in Cuprate Superconductors at a Lifshitz Transition, *Phys. Rev. Lett.* **114**, 147001 (2015).
- [33] W. Wu, M. S. Scheurer, S. Chatterjee, S. Sachdev, A. Georges, and M. Ferrero, Pseudogap and Fermi-Surface Topology in the Two-Dimensional Hubbard Model, *Phys. Rev. X* **8**, 021048 (2018).
- [34] N. Doiron-Leyraud *et al.*, Pseudogap phase of cuprate superconductors confined by Fermi surface topology, *Nat. Commun.* **8**, 2044 (2017).
- [35] J. G. Storey, J. L. Tallon, and G. V. M. Williams, Thermodynamic properties of  $Bi_2Sr_2CaCu_2O_8$  calculated from the electronic dispersion, *Phys. Rev. B* **77**, 052504 (2008).
- [36] Y. Zhong, Z. Chen, S.-D. Chen, K.-J. Xu, M. Hashimoto, Y. He, S.-I. Uchida, D. Lu, S.-K. Mo, and Z.-X. Shen, Differentiated roles of Lifshitz transition on thermodynamics and superconductivity in  $La_{2-x}Sr_xCuO_4$ , *Proc. Natl. Acad. Sci. USA* **119**, e2204630119 (2022).
- [37] M. Horio, K. Hauser, Y. Sassa, Z. Mingazheva, D. Sutter, K. Kramer, A. Cook, E. Nocerino, O. K. Forslund, O. Tjernberg, M. Kobayashi, A. Chikina, N. B. M. Schroter, J. A. Krieger, T. Schmitt, V. N. Strocov, S. Pyon, T. Takayama, H. Takagi, O. J. Lipscombe, S. M. Hayden, M. Ishikado, H. Eisaki, T. Neupert, M. Mansson, C. E. Matt, and J. Chang, Three-Dimensional Fermi Surface of Overdoped La-Based Cuprates, *Phys. Rev. Lett.* **121**, 077004 (2018).
- [38] I. K. Drozdov, I. Pletikosić, C.-K. Kim, K. Fujita, G. D. Gu, J. C. Séamus Davis, P. D. Johnson, I. Božović, and T. Valla, Phase diagram of  $Bi_2Sr_2CaCu_2O_{8+\delta}$  revisited, *Nat. Commun.* **9**, 5210 (2018).
- [39] Y. He, S. D. Chen, Z. X. Li, D. Zhao, D. Song, Y. Yoshida, H. Eisaki, T. Wu, X. H. Chen, D. H. Lu, C. Meingast, T. P. Devereaux, R. J. Birgeneau, M. Hashimoto, D. H. Lee, and Z.-X. Shen, Superconducting Fluctuations in Overdoped  $Bi_2Sr_2CaCu_2O_{8+\delta}$ , *Phys. Rev. X* **11**, 031068 (2021).
- [40] M. P. Allen *et al.*, Formation of heavy  $d$ -electron quasiparticles in  $Sr_3Ru_2O_7$ , *New J. Phys.* **15**, 063029 (2013).
- [41] H. Padamsee, J. E. Neighbor, and C. A. Shiffman, Quasiparticle phenomenology for thermodynamics of strong-coupling superconductors, *J. Low Temp. Phys.* **12**, 387 (1973).
- [42] J. W. Loram, K. A. Mirza, and J. R. Cooper, Properties of the superconducting condensate and normal-state pseudogap in



- high- $T_c$  superconductors derived from the electronic specific heat, in *IRC in Superconductivity Research Review* (Cambridge University, Cambridge, 1998).
- [43] J. W. Loram, K. A. Mirza, J. M. Wade, J. R. Cooper, and W. Y. Liang, The electronic specific heat of cuprate superconductors, *Physica C* **235-240**, 134 (1994).
- [44] J. G. Storey, J. L. Tallon, and G. V. M. Williams, Pseudogap ground state in high-temperature superconductors, *Phys. Rev. B* **78**, 140506(R) (2008).
- [45] T. Nakano, M. Oda, C. Manabe, N. Momono, Y. Miura, and M. Ido, Magnetic properties and electronic conduction of superconducting  $\text{La}_{2-x}\text{Sr}_x\text{CuO}_4$ , *Phys. Rev. B* **49**, 16000 (1994).
- [46] A. Dubroka, M. Rossle, K. W. Kim, V. K. Malik, D. Munzar, D. N. Basov, A. A. Schafgans, S. J. Moon, C. T. Lin, D. Haug, V. Hinkov, B. Keimer, T. Wolf, J. G. Storey, J. L. Tallon, and C. Bernhard, Evidence of a Precursor Superconducting Phase at Temperatures as High as 180 K in  $\text{RBa}_2\text{Cu}_3\text{O}_{7-\delta}$  ( $R = \text{Y}, \text{Gd}, \text{Eu}$ ) Superconducting Crystals from Infrared Spectroscopy, *Phys. Rev. Lett.* **106**, 047006 (2011).